Lawrence Berkeley National Laboratory

Lawrence Berkeley National Laboratory

Title

Sum Frequency Generation Vibrational Spectroscopy of Pyridine Hydrogenation on Platinum Nanoparticles

Permalink

https://escholarship.org/uc/item/5zw640v1

Author

Bratlie, Kaitlin M.

Publication Date

2009-01-21

eScholarship.org Powered by the California Digital Library
University of California

Sum Frequency Generation Vibrational Spectroscopy of Pyridine Hydrogenation on Platinum Nanoparticles

Kaitlin M. Bratlie,[1,2,‡] Kyriakos Komvopoulos,[2] and Gabor A. Somorjai[1,*]

AUTHORS ADDRESSES:

[1]Department of Chemistry, University of California, Berkeley, California 94720, and

Materials Sciences Division, Lawrence Berkeley National Laboratory, Berkeley, California 94720

[2]Department of Mechanical Engineering, University of California, Berkeley, California 94720

AUTHOR EMAIL ADDRESS: somorjai@berkeley.edu

RECEIVED DATE

TITLE RUNNING HEAD: Pyridine hydrogenation on Pt nanoparticles

CORRESPONDING AUTHOR FOOTNOTE

[*]Corresponding author: Tel: 510-642-4053; Fax: 510-643-9668; E-mail: somorjai@berkeley.edu

[‡]Current address: David H. Koch Institute for Integrative Cancer Research, Massachusetts Institute of Technology, 77 Massachusetts Avenue, Cambridge, MA 02139.

ABSTRACT

Pyridine hydrogenation in the presence of a surface monolayer consisting of cubic Pt nanoparticles stabilized by tetradecyltrimethylammonium bromide (TTAB) was investigated by sum frequency generation (SFG) vibrational spectroscopy using total internal reflection (TIR) geometry. TIR-SFG spectra analysis revealed that a pyridinium cation ($C_5H_5NH^+$) forms during pyridine hydrogenation on the Pt nanoparticle surface, and the NH group in the $C_5H_5NH^+$ cation becomes more hydrogen bound with the increase of the temperature. In addition, the surface coverage of the cation decreases with the increase of the temperature. An important contribution of this study is the *in situ* identification of reaction intermediates adsorbed on the Pt nanoparticle monolayer during pyridine hydrogenation.

KEYWORDS. Heterogeneous catalysis, platinum, nanoparticles, pyridine, hydrogenation, sum frequency generation spectroscopy.

1. Introduction

Basic understanding of catalysis at the molecular level has been the central objective of several recent investigations.[1-4] Identification of surface intermediates during catalysis is of critical importance in understanding nanoscale catalytic processes. Bridging the materials gap from single crystals to nanoparticles is crucial in elucidating catalysis phenomena encountered in industrially relevant processes. Pyridine (C_5H_5N) is a simple aromatic organic compound structurally related to benzene (one CH group in the six-member ring is replaced by a nitrogen atom) and is an important building block, solvent, and reagent in organic synthesis. Since the lone pair of electrons at the nitrogen atom is not delocalized into the aromatic π-system, pyridine is electron donating and exhibits chemical properties similar to those of tertiary amines.

Pyridine is protonated by reaction with acids and forms a positively charged aromatic polyatomic ion known as pyridinium cation ($C_5H_5NH^+$). This cation is of particular interest because of its distinct vibrational signature compared to other adsorbates forming during pyridine hydrogenation.[5] Another desirable effect is that the formation of pyridinium cations is thermodynamically favorable on platinum surfaces.[5] At a high surface coverage, pyridine adsorbs with the aromatic ring perpendicular to the metal surface through the nitrogen and adjacent carbon atoms in an *α*-pyridyl structure,[6] preventing complete hydrogenation of the ring.

The main objective of this study was to examine surface intermediates during pyridine hydrogenation on monolayers consisting of cubic Pt nanoparticles stabilized by a very thin layer of tetradecyltrimethylammonium bromide (TTAB) under conditions of 10 Torr C_5H_5N, 100 Torr H_2, and 650 Torr Ar in the temperature range of 300–400 K. This is the first study to provide evidence of a reactive intermediate on a nanoparticle monolayer surface during nanoscale catalysis.

Electron spectroscopy typically cannot be used under ambient pressure conditions of catalytic reactions. Sum frequency generation (SFG) vibrational spectroscopy is a much more effective technique for interface chemical analysis than infrared (IR) absorption and Raman spectroscopy because the SFG signal arises solely from the adsorbates. Materials with centrosymmetry and isotropic gases do not

appear in the SFG spectrum under the electric dipole approximation. Since bulk Pt has a center of inversion, its contribution to the SFG signal is negligible. Furthermore, a surface specific signal is produced because symmetry is broken at the surface of a Pt crystal. Therefore, SFG spectroscopy and total internal reflection (TIR) geometry were used to study pyridine hydrogenation on a monolayer consisting of Pt nanoparticles in a relatively high temperature range (300–400 K), the main objective being the identification of reactive intermediates during pyridine hydrogenation.

2. Experimental Procedures

2.1. Synthesis and Assembly of Platinum Nanoparticles

Cubic nanoparticles stabilized with TTAB were prepared by mixing aqueous solutions of K_2PtCl_4 (99.9% pure, Alfa Aesar) and TTAB (99% pure, Aldrich) in a 20 mL vial at room temperature.[7] The mixture was heated to 323 K for ~5 min until the solution became clear. After the addition of ice-cold $NaBH_4$ (98% pure, Strem Chemicals), the vial was capped with a rubber septum and the H_2 gas pressure inside the vial was released through a needle in the septum for 10 min. After the removal of the needle, the solution was kept at 323 K for 6 h. The cubic nanoparticles were prepared from a solution consisting of 100 mM TTAB and 1 mM K_2PtCl_4 reduced with 30 mM $NaBH_4$. First, the nanoparticles were centrifuged at 3 krpm for 30 min and the precipitates were discarded. Then, the solution was centrifuged again at 14 krpm for 10 min, the supernatant was discarded, and the precipitates were re-dispersed in deionized (DI) water by sonication. Finally, the solution was once again centrifuged at 14 krpm for 10 min, and the precipitates were collected and re-dispersed in DI water. The washed nanoparticles were used in transmission electron microscope (TEM) analysis and reaction studies. The shape and size distributions of the synthesized cubic nanoparticles were studied in a TEM (JEOL 200CX) operated at 200 kV.

For spectroscopic measurements, cubic nanoparticles were deposited on a fused quartz prism, using the Langmuir-Blodgett (LB) technique. Colloidal Pt solutions were dispersed on the surface of DI water (18 MΩ·cm) sub-phase on a LB trough (type 611, NIMA Technology) at room temperature. The

surface pressure (monitored with a Wilhelmy plate) was set equal to zero before spreading the nanoparticles. The resulting surface layer was compressed by a mobile barrier at a rate of 20 cm^2/min. The nanoparticles were deposited by lifting the prism that had been immersed in water sub-phase prior to dispersing the nanoparticles at a surface pressure of ~20 mN/m. Representative TEM images of the nanoparticles used in this study have been presented elsewhere.[7,8] These images show that these cubic Pt nanoparticles do not exhibit any observable tilting with respect to the prism surface.

2.2. Reaction Cell

A custom-made cell was used for *in-situ* SFG spectroscopy in TIR geometry under batch gas circulation. A fused quartz prism coated with a nanoparticle monolayer was pressed against a rubber O-ring by tightening a teflon block with two set screws. The temperature at the prism surface was measured with a thermocouple placed directly onto the sample. Heating was applied by wrapping the reactor cell with a heat tape (McMaster-Carr) and applying a variable voltage. Temperature variations across the 20 × 20 mm^2 prism area were insignificant. The reaction cell was connected to a stainless steel tubing gas manifold of diameter equal to 0.3175 cm. Pyridne ($\geq$99.8 wt%, Fluka) was purified by several freeze-pump-thaw cycles before being introduced into the reaction cell. Before each experiment, pyridine was checked for impurities by gas chromatography (GC). Impurity levels were found to be less than 0.5 wt% and consisted of mostly light alkanes below C_6. A vacuum pressure of less than 1 mTorr was maintained in the reaction cell by mechanical and turbomolecular pumps.

2.3. Sum Frequency Generation

A mode-locked Nd:YAG laser with a 1064 nm fundamental wavelength and a 20 ps pulse width operated at a 20 Hz repetition rate was used to generate a tunable IR (2750–3600 cm^{-1}) beam and a 532-nm second harmonic visible (VIS) beam in the SFG experiments. The IR and VIS beams (25 and 50 μJ, respectively) were spatially and temporally overlapped on the fused quartz surface at incident angles of 55º and 60º with respect to the surface normal. SFG-TIR spectra were obtained using *ppp* (i.e., SFG, VIS, and IR beams all p-polarized) and *ssp* polarization combinations. The SFG beam was passed

through a monochromator, and the signal intensity was detected with a photomultiplier tube and a gated integrator while the IR beam was scanned over the frequency range of interest. Because gas molecules absorb some of the incoming radiation, the SFG output was normalized by the intensity of the incident IR beam at the surface. Curve fitting of the SFG-TIR spectra was based on a previously reported procedure,[9,10] using the following relationship:

$$I_{SFG} \propto \left| \chi_{NR}^{(2)} e^{i\phi_{NR}} + \sum_q \frac{A_q}{\omega_{IR} - \omega_q + i\Gamma_q} e^{i\gamma_q} \right|^2 \quad (1)$$

where $\chi_{NR}^{(2)}$ is the nonresonant nonlinear susceptibility, ϕ_{NR} is the phase associated with the nonresonant background, A_q is the strength of the qth vibrational mode, ω_{IR} is the frequency of the incident IR laser beam, ω_q is the frequency of the qth vibrational mode, Γ_q is the natural line width of the qth vibrational transition, and γ_q is the phase associated with the qth vibrational transition. Detailed descriptions of SFG theory can be found elsewhere.[11-16]

3. Results and Discussion

Monolayers of TTAB-stabilized Pt nanoparticles were used in the pyridine hydrogenation experiments. The nanoparticles (79% cubes, 3% triangles, and 18% irregular shapes) consisted of only Pt(100) and were 12.3 ± 1.4 nm in size (diagonal). Figure 1 shows SFG spectra (*ssp* polarization) of a monolayer consisting of TTAB-stabilized cubic Pt nanoparticles obtained before the introduction of pyridine (Figure 1(a)) and during pyridine hydrogenation (10 Torr C_5H_5N, 100 Torr H_2, and 650 Torr Ar) at 300 K (Figure 1(b)) and 325 K (Figure 1(c)). Corresponding peak assignments are given in Table 1. The peaks at 2845 and 2935 cm^{-1} are attributed to symmetric and asymmetric methylene stretches [CH_2(s) and CH_2(a), respectively], the peaks at 2870 and 2955 cm^{-1} are assigned to symmetric and asymmetric methyl stretches [CH_3(s) and CH_3(a), respectively], while the peak at 2900 cm^{-1} is attributed to the CH_2, $C–H_{distal}$ stretch. After the introduction of pyridine, an additional peak appeared at 3050 cm^{-1}. This peak is assigned to the aromatic –C=C–H stretch arising from pyridine adsorbed to the Pt surface.

Figure 2 shows SFG spectra (*ppp* polarization) of a monolayer consisting of TTAB-stabilized cubic Pt nanoparticles obtained before and after pyridine hydrogenation. The SFG spectrum at the bottom of this figure (acquired before the introduction of pyridine to eliminate the stabilizing agent as a possible source of SFG signal) is featureless in the wavelength range of 3300–3550 cm^{-1}. However, a peak indicative of the pyridinium cation[5] appeared at 3450 cm^{-1} after the introduction of pyridine in the presence of hydrogen. The temperature increase resulted in slight red-shifting of the N–H peak at 3450 cm^{-1}, possibly indicating an increase in the hydrogen bonding of the NH bonds. This apparent red-shift may also arise from the upcoming N–H peak resulting from the temperature rise. As the temperature is increased, the adsorbed pyridine may not be as easily protonated, resulting in the appearance of the N–H peak.

Surface coverage σ (molecules/cm^2) by an adsorbate is defined as

$$\sigma = F\tau, \tag{2}$$

where F is the incident flux (molecules/cm^2/s) and τ is the residence time given by

$$\tau = \tau_0 \exp\left(\frac{\Delta H_{ads}}{RT}\right), \tag{3}$$

where τ_0 is correlated to the surface atom vibration time (typically 10^{-12} s), ΔH_{ads} is the heat of adsorption, T is the temperature, and R is the gas constant. According to Eq. (3), surface coverage by an adsorbate decreases exponentially with the increase of the temperature. Hence, the decrease of the peak intensity with the temperature, shown in Figure 2, may be associated with the reduced surface coverage at higher temperatures.

Figure 3 shows *ssp* and *ppp* polarized SFG spectra of a monolayer consisting of TTAB-stabilized Pt nanoparticles obtained during pyridine hydrogenation (10 Torr C_5H_5N, 100 Torr H_2, and 650 Torr Ar). In the *ssp* spectrum (Figure 3(a)), a new peak appears at 3400 cm^{-1} and is assigned to a N–H stretch.[17,18] The two-fold increase of the signal intensity in the *ppp* spectrum (Figure 3(b)) suggests that the pyridinium cation is oriented parallel to the surface normal of the prism. It should be noted that this

does not necessarily imply that the adsorbate is parallel to the nanoparticle surface normal, since the resulting signal may arise from the top of the nanoparticle as well as its sides. For example, if the pyridinium cation were to adsorb in a flat-laying conformation on the nanoparticle sides, the intensity of the *ppp* spectrum would have been higher than that of the *ssp* spectrum since the adsorbate would be still parallel to the surface normal of the prism. Earlier studies of pyridine adsorption on Pt single crystals have shown that at a high coverage (>0.6 ML) pyridine adsorbs in an upright conformation, parallel to the surface normal.[19-21] The pyridinium cation has also been suggested to adopt an upright or tilted conformation, as shown in Figure 4.[5] Determining the orientation of the adsorbed pyridinium relative to the nanoparticle surface is complex due to the exponential decay of the electric field resulting from the TIR geometry. Consequently, the SFG field may be different on opposite nanoparticle sides, breaking the inversion symmetry.[22] Assuming that inversion symmetry holds, the top nanoparticle surface will be the dominant contributor to the SFG signal and the pyridinium cation will be oriented in an upright conformation, as shown schematically in Figure 4.

4. Conclusions

Pyridine hydrogenation on a monolayer consisting of TTAB-stabilized cubic Pt nanoparticles investigated by TIR-SFG spectroscopy revealed the adsorption of a pyridinium cation intermediate under conditions of 10 Torr C_5H_5N, 100 Torr H_2, and 650 Torr Ar. The NH group in the pyridinium cation became more hydrogen bound with the increase of the temperature, as suggested by a red-shift in the N–H peak, while the decrease in the intensity of this peak at elevated temperatures indicated a decrease in surface coverage of the pyridinium cation. A novel contribution of this study is the *in situ* identification of reactive intermediates on Pt nanoparticle monolayers during catalytic reactions.

Acknowledgment. This work was supported by the Berkeley-ITRI Research Center (BIRC) under Fund No. 46101-23845-44-EKMAJ, and the Director, Office of Energy Research, Office of Basic Energy Sciences, and Materials Science Division of the U.S. Department of Energy under Contract No. DE-

AC02-05CH11231. The authors are grateful to S. Habas and Professor P. Yang for nanoparticle monolayer synthesis.

References and Notes

(1) Somorjai, G. A. *Journal of Molecular Catalysis A: Chemical* **1996**, *107*, 39-53.

(2) Zaera, F. *Progress in Surface Science* **2001**, *69*, 1-98.

(3) LeBlanc, R. J.; Chu, W.; Williams, C. T. *Journal of Molecular Catalysis A: Chemical* **2004**, *212*, 277-289.

(4) Williams, C. T.; Yang, Y.; Bain, C. D. *Langmuir* **2000**, *16*, 2343-2350.

(5) Lee, I. C.; Masel, R. I. *Journal of Physical Chemistry B* **2002**, *106*, 368-373.

(6) Connolly, M.; Somers, J.; Bridge, M. E.; Lloyd, D. R. *Surface Science* **1987**, *185*, 559-568.

(7) Lee, H.; Habas, S. E.; Kweskin, S. J.; Butcher, D.; Somorjai, G. A.; Yang, P. *Angewandte Chemie-International Edition* **2006**, *45*, 7824-7828.

(8) Bratlie, K. M.; Lee, H.; Komvopoulos, K.; Yang, P.; Somorjai, G. A. *Nano Letters* **2007**, *7*, 3097-3101.

(9) Bain, C. D.; Davies, P. B.; Ong, T. H.; Ward, R. N.; Brown, M. A. *Langmuir* **1991**, *7*, 1563-1566.

(10) Moore, F. G.; Becraft, K. A.; Richmond, G. L. *Applied Spectroscopy* **2002**, *56*, 1575-1578.

(11) Kung, K. Y.; Chen, P.; Wei, F.; Rupprechter, G.; Shen, Y. R.; Somorjai, G. A. *Review of Scientific Instruments* **2001**, *72*, 1806-1809.

(12) Yang, M.; Tang, D. C.; Somorjai, G. A. *Review of Scientific Instruments* **2003**, *74*, 4554-4557.

(13) Bratlie, K. M.; Flores, L. D.; Somorjai, G. A. *Surface Science* **2005**, *599*, 93-106.

(14) Shen, Y. R. *The Principles of Nonlinear Optics*; Wiley: New York, 2003.

(15) Shen, Y. R. *Annual Review of Physical Chemistry* **1989**, *40*, 327-350.

(16) Shen, Y. R. *Nature* **1989**, *337*, 519-525.

(17) Kang, D. H.; Trenary, M. *Surface Science* **2000**, *470*, L13-L19.

(18) Kang, D. H.; Trenary, M. *Surface Science* **2002**, *519*, 40-56.

(19) Horsley, J. A.; Stohr, J.; Hitchcock, A. P.; Newbury, D. C.; Johnson, A. L.; Sette, F. *Journal of Chemical Physics* **1985**, *83*, 6099-6107.

(20) Haq, S.; King, D. A. *Journal of Physical Chemistry* **1996**, *100*, 16957-16965.

(21) Grassian, V. H.; Muetterties, E. L. *Journal of Physical Chemistry* **1987**, *91*, 389-396.

(22) Yeganeh, M. S.; Dougal, S. M.; Silbernagel, B. G. *Langmuir* **2006**, *22*, 637-641.

List of Tables and Figures

Table 1. Peak assignments in SFG spectra of a monolayer consisting of TTAB-stabilized cubic Pt nanoparticles obtained before and during pyridine hydrogenation (10 Torr C_5H_5N, 100 Torr H_2, 650 Torr Ar, and temperature in the range of 300–400 K).

Figure 1. SFG spectra (*ssp* polarization) of a monolayer consisting of TTAB-stabilized cubic Pt nanoparticles obtained (a) before and (b),(c) during pyridine hydrogenation (10 Torr C_5H_5N, 100 Torr H_2, and 650 Torr Ar) at (b) 300 K and (c) 325 K. Markers represent experimental data and solid lines curve fits that follow Eq. (1).

Figure 2. SFG spectra (*ppp* polarization) of a monolayer consisting of TTAB-stabilized cubic Pt nanoparticles showing the pyridinium $N–H^+$ band before (bottom spectrum) and during pyridine hydrogenation (10 Torr C_5H_5N, 100 Torr H_2, 650 Torr Ar, and temperature in the range of 300–400 K). Markers represent experimental data and solid lines curve fits that follow Eq. (1).

Figure 3. SFG spectra of a monolayer consisting of TTAB-stabilized cubic Pt nanoparticles for (a) *ssp* and (b) *ppp* polarization. The spectra show the pyridinium $N–H^+$ and N–H bands during pyridine hydrogenation (10 Torr C_5H_5N, 100 Torr H_2, 650 Torr Ar, and temperature of 300 K). Markers represent experimental data and solid lines curve fits that follow Eq. (1).

Figure 4. Schematic diagram of two possible configurations of the pyridinium cation ($C_5H_5NH^+$) intermediate. The green, gray, and blue spheres represent carbon, hydrogen, and nitrogen atoms, respectively.

Table 1. Peak assignments in SFG spectra obtained from a monolayer consisting of TTAB-stabilized cubic Pt nanoparticles before and after pyridine hydrogenation under conditions of 10 Torr C_5H_5N, 100 Torr H_2, 650 Torr Ar, and temperature in the range of 300–400 K.

Wavenumber (cm^{-1})	Peak assignment (surface)
3450	$N–H^+$ (pyridine)
3400	N–H (pyridine)
3050	–C=C–H (pyridine)
2955	CH_3(a) (TTAB)
2935	CH_2(a) (TTAB)
2900	CH_2, $C–H_{distal}$ (TTAB)
2870	CH_3(s) (TTAB)
2845	CH_2(s) (TTAB)

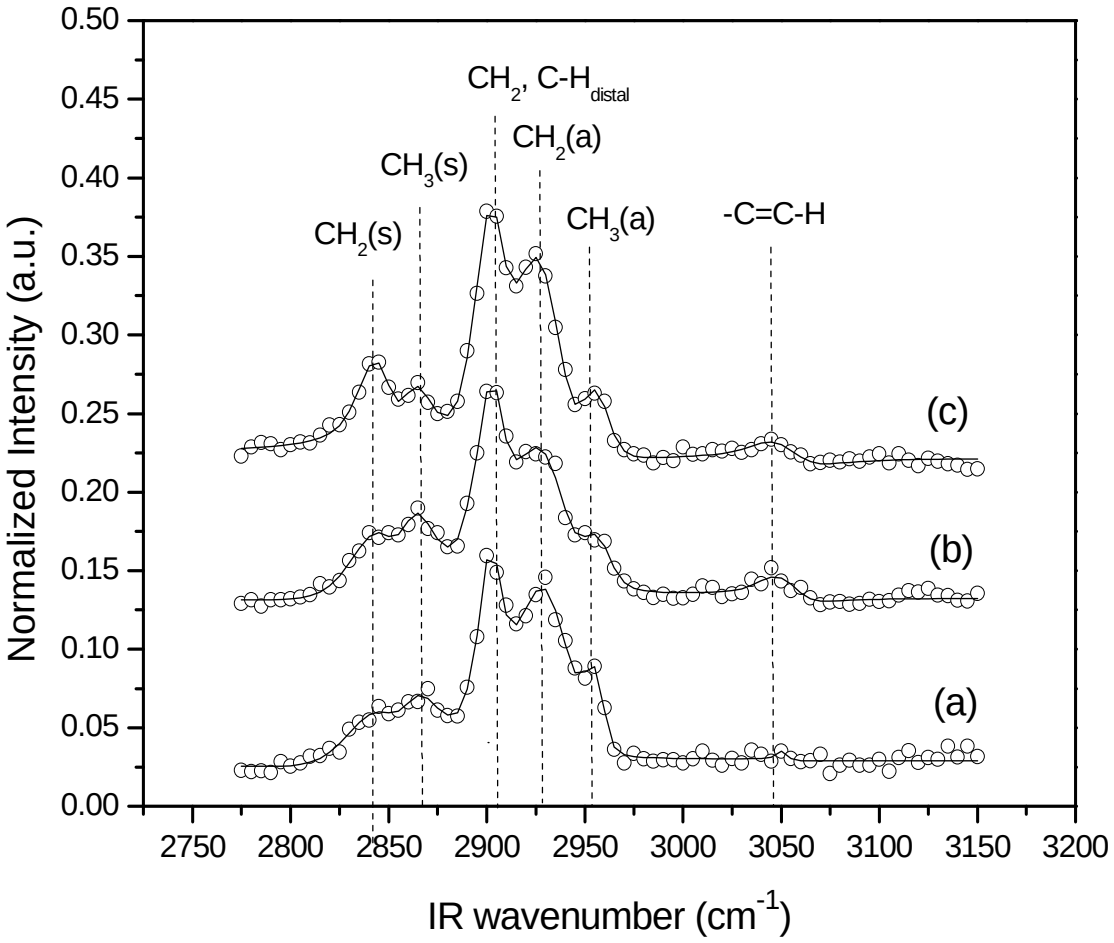
0.50
0.45
0.40
0.35
0.30
0.25
0.20
0.15
0.10
0.05
0.00
Normalized Intensity (a.u.)
CH2, C-Hdistal
CH2(a)
CH3(s)
CH2(s)
CH3(a)
-C=C-H
(c)
(b)
(a)
2750
2800
2850
2900
2950
3000
3050
3100
3150
3200
IR wavenumber (cm-1)

Figure 1

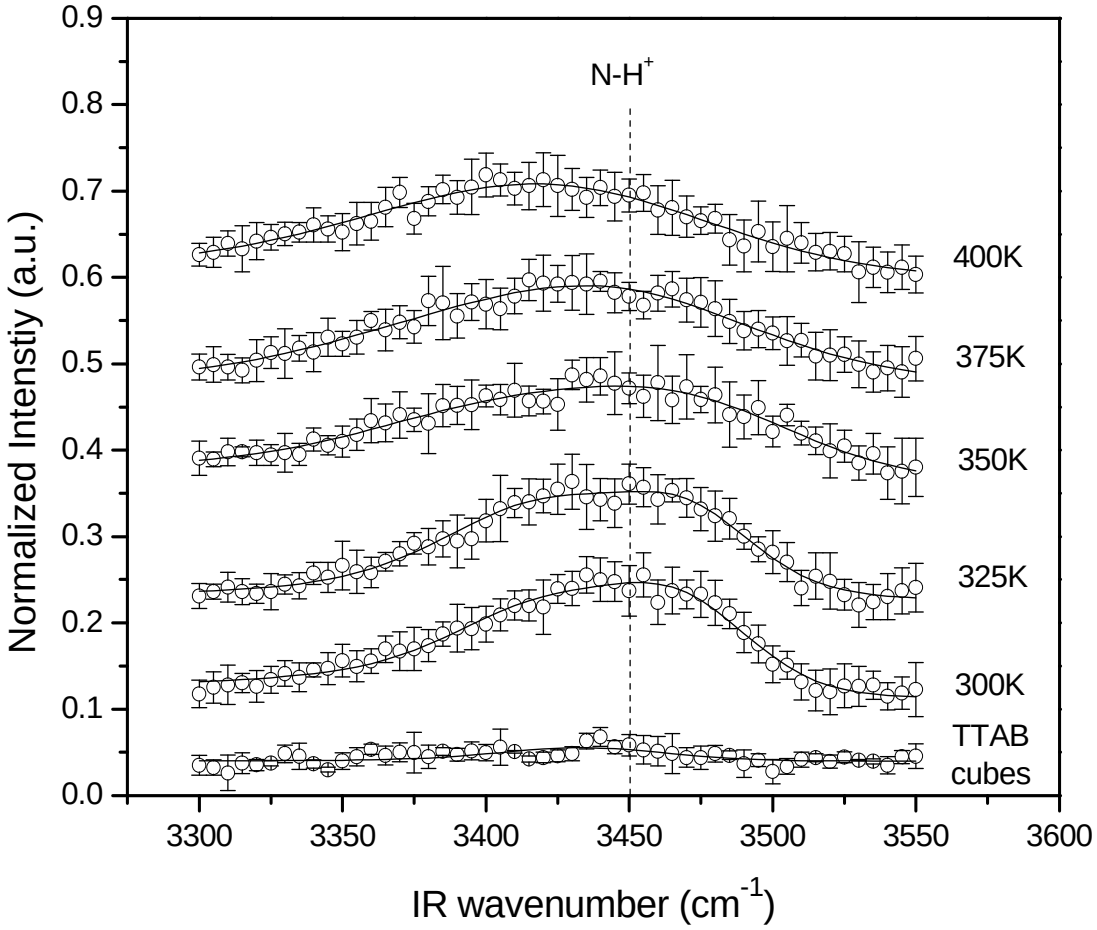
N-H+
400K
375K
350K
325K
300K
TTAB
cubes
Normalized Intenstiy (a.u.)
IR wavenumber (cm-1)
0.0
0.1
0.2
0.3
0.4
0.5
0.6
0.7
0.8
0.9
3300
3350
3400
3450
3500
3550
3600

Figure 2

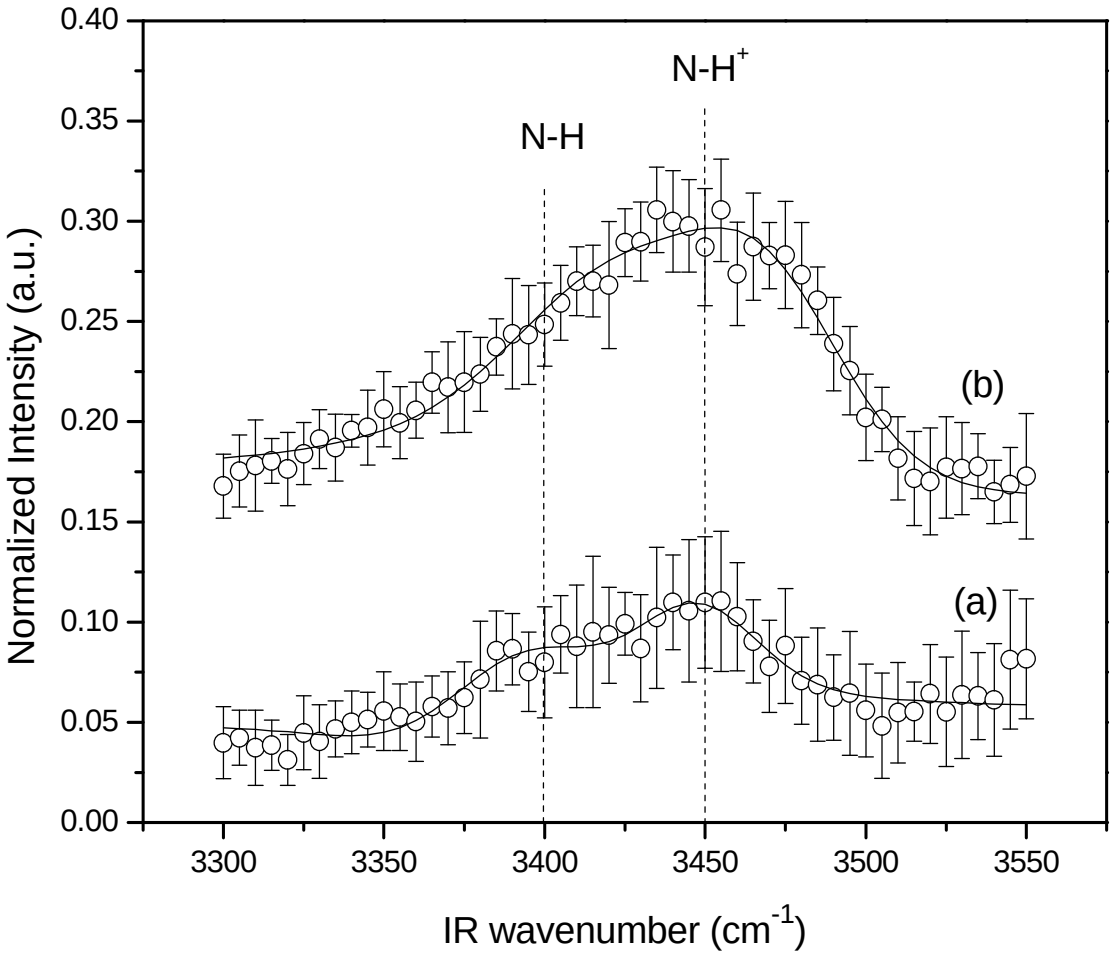
0.40
0.35
0.30
0.25
0.20
0.15
0.10
0.05
0.00
Normalized Intensity (a.u.)
N-H+
N-H
(b)
(a)
3300
3350
3400
3450
3500
3550
IR wavenumber (cm-1)

Figure 3

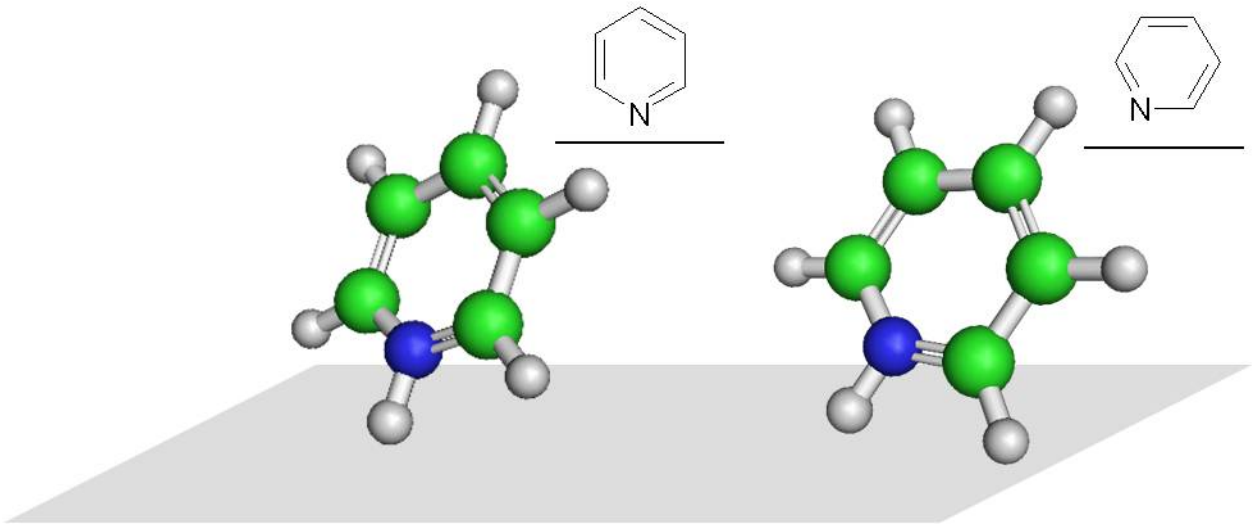

Figure 4